Statistical Properties of Distribution of Solid Particles at the Bottom Setting in Turbulent Shear Flow

AUTHOR(S):

NAKAGAWA, Hiroji; OTSUBO, Kuninori

CITATION:

NAKAGAWA, Hiroji ...[et al]. Statistical Properties of Distribution of Solid Particles at the Bottom Setting in Turbulent Shear Flow. Memoirs of the Faculty of Engineering, Kyoto University 1979, 41(2): 74-95

ISSUE DATE:

1979-06-30

URL:

http://hdl.handle.net/2433/281094

Statistical Properties of Distribution of Solid Particles at the Bottom Setting in Turbulent Shear Flow

By

Hiroji NAKAGAWA*, and Kuninori OTSUBO**

(Received December 19, 1978)

Abstract

In this paper the behaviors of settling particles in turbulent shear flow are investigated and the statistical properties of distribution of the particles at the bottom are obtained experimentally and theoretically. For the properties of distribution of the particles, the mean settling length of the particle, that is, the mean value of the streamwisely transported length of the particle, and the standard deviation of the settling length are considered. These statistical properties are obtained by experiment and the trajectories of the settling particles are photographed by storoboscopic light. Then, on the basis of these experimental results, the stochastic models for the behaviors of the settling particles are developed. These models can explain well the actual phenomena, and it is found that these stochastic models are to be pertinent. Problems to be solved in the future are discussed.

1. Introduction

A local scour around the bridge pier is caused by high shear near the bed. The high shear is produced by a horseshoe vortex caused by a flow separation which occurs near the pier due to a pressure increase owing to the presence of the pier. It is well-known that the rubble mount method is effective to reduce the local scour and protect the bed around the pier. The principle of the rubble mount method is to cover the bed by large scale rubbles, which make a critical shear stress larger than a flow shear stress acting on the bed. In a deep ocean cannal with a high flow velocity, the protection work at the bottom is very difficult. In this case, the rubble mount method is easy and inexpensive, since the rubble is simply dumped from a ship or official platform. But, when the rubble falls in the turbulent shear flow, it oscillates and fluctuates, due to the flow fluctuation and vorticies behind the rubble itself. Hence, when it reaches the bed, its longitudinal transported length is considerably dispersed. In order to execute the

* Department of Civil Engineering.
** Department of Civil Engineering.
Present address: National Institute for Environmental Studies.

rubble mount method effectively and economically, rubble must be distributed properly at the appointed region on the bottom. Therefore, it is necessary to make clear the property of distribution of the falling particles.

Extensive experiments were conducted in order to understand the physical behavior of the falling particles in turbulent shear flow and the distributional properties of particles on the bottom bed. Based on these experiments the statistical properties of particle distribution are analyzed by using the mean settling length and the deviation of its length. These statistical properties are expressed as a function of the mean velocity, depth, characteristics of particles such as the settling velocity and the shape factor, etc..

We propose a stochastic model for the behavior of the settling particle. Using this model, the relations between the mean settling length, the standard deviation of its length and depth, the mean velocity and the settling velocity are investigated. The details are discussed in the following sections.

2. Experimental Setup

The flume used for this experiment was 15 m long, 0.5 m wide and 1 m deep, and was made of steel, but the sides of the flume were made of glass 1 cm thick. Then we could execute the stroboscopic photographing.

In order to measure the transported length of a particle, which fell in turbulent shear flow and reached the bottom, we used the collecting box. This box is 5 cm in depth and 30 cm $\times$ 30 cm square, and longitudinally it is divided at 1 cm intervals and transversely divided at 16/15 cm intervals. This box was set up on the flume, such that the top of this box was level at the bottom. The particles were dumped from the appointed point at the free surface. After the particles had been dumped N times, we pulled up this box and counted the number of particles at every section.

Experimental runs of series P, B and F are summarized in Table 1. Series P indicates the experiments in which one particle is dumped by a pincette, and in series B, particles are dumped by a bucket. Series F indicates the experiments for photographs, in which one particle dumped by a pincette is shot on storoboscopic light. The particles used are beads of 5 mm and 7 mm diameters, an iron ball of 5 mm diameter and gravel of 4.5 mm mean diameter. The flow depth of series P and B are 20, 35 and 50 cm, and u_0 is the mean velocity at the section.

In Table 1, N is the number of trials, in a word, the number of settling exercises, and m is the number of particles dumped at one trial. In series B, the particles are dumped by a bucket, and then m is 1 or 5 or 10, but mainly 10. The photograph of the bucket used in this experiment is shown in Photo. 1.

In order to investigate the behavior of one particle falling in turbulent shear flow, we introduced the photographic method such that the particle was shot on storoboscopic

Table 1. Experimental Setup

Run	Mean Velocity u_0 (cm/s)	Water Depth H (cm)	Particle	m	N
P-1	0.0	20.0	Bead	1	150
P-2	10.0		d=0.5 cm		150
P-3	15.2				150
P-4	25.3				150
P-5	0.0	35.0			150
P-6	10.0				150
P-7	15.2				200
P-8	25.3				150
P-9	0.0	50.0			150
P-10	10.0				150
P-11	15.2				150
P-12	25.3				150
P-13	0.0	20.0	Gravel	1	150
P-14	10.0		d=0.45 cm		150
P-15	15.2				150
P-16	25.3				150
P-17	0.0	35.0			150
P-18	10.0				200
P-19	15.2				250
P-20	25.3				250
P-21	0.0	50.0			250
P-22	10.0				200
P-23	15.2				200
P-24	25.3				250
P-25	15.2	35.0	Bead	1	200
P-26	15.2	50.0	d=0.5 cm		200
P-27	15.2	35.0	Gravel	1	200
P-28	15.2	50.0	d=0.5 cm		200
F-1	10.0	20.0	Bead	1	15
F-2	15.2		d=0.5 cm		15
F-3	25.3				15
F-4	10.0	50.0			150
F-5	15.2				150
F-6	25.3				160
F-7	10.0	20.0	Gravel	1	15
F-8	15.2		d=0.5 cm		15
F-9	25.3				15
F-10	10.0	50.0			130
F-11	15.2				150
F-12	25.3				160
F-13	25.3	50.0	B. (0.7)	1	130
F-14	25.3	50.0	I. (0.5)	1	20
F-15	0.0	60.0	B. (0.5)	1	10
F-16	0.0	60.0	G. (0.45)	1	10

Run	Mean Velocity u_0 (cm/s)	Water Depth H (cm)	Particle	m	N
B-1	0.0	20.0	Beads	1	200
B-2	0.0		d=0.5 cm	5	100
B-3	0.0			10	100
B-4	10.0			1	200
B-5	10.0			5	100
B-6	10.0			10	100
B-7	15.2			1	200
B-8	15.2			5	100
B-9	15.2			10	100
B-10	25.3			1	200
B-11	25.3			5	100
B-12	25.3			10	100
B-13	0.0	35.0		10	100
B-14	10.0			10	100
B-15	15.2			1	200
B-16	15.2			5	100
B-17	15.2			10	100
B-18	25.3			10	100
B-19	0.0	50.0		10	100
B-20	10.0			10	100
B-21	15.2			1	200
B-22	15.2			5	125
B-23	15.2			10	100
B-24	25.3			10	100
B-25	0.0	20.0	Gravel	10	100
B-26	0.0		d=0.45 cm	5	125
B-27	0.0			10	100
B-28	10.0			1	200
B-29	10.0			5	125
B-30	10.0			10	100
B-31	15.2			1	200
B-32	15.2			5	125
B-33	15.2			10	100
B-34	25.3			1	200
B-35	25.3			5	125
B-36	25.3			10	100
B-37	0.0	35.0		10	100
B-38	15.2			10	100
B-39	15.2			1	200
B-40	10.0			5	125
B-41	15.2			10	100
B-42	25.3			10	100
B-43	0.0	50.0		10	100
B-44	10.0			10	100
B-45	15.2			1	200
B-46	15.2			5	125
B-47	15.2			10	100
B-48	25.3			10	100

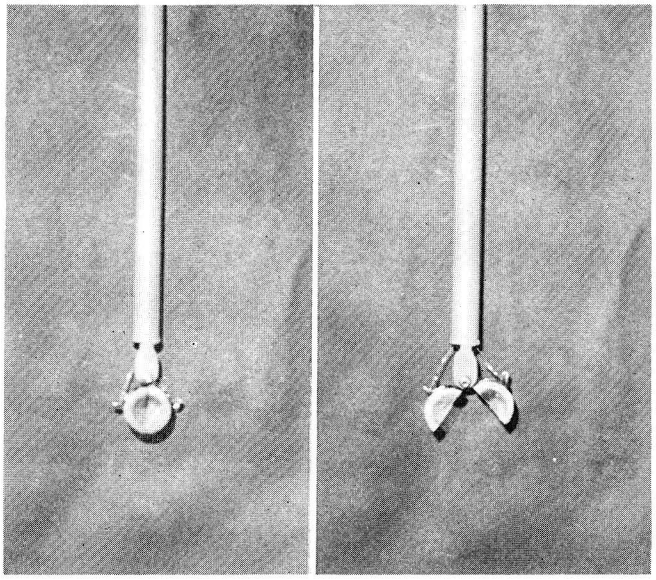

Photo. 1. Bucket for particle dumping.

light. The principle of this method is such that we irradiate storoboscopic light to a falling particle at some constant intervals in a dark space. Then the falling particle trajectory can be seen as a spotted line, and we can photograph this spotted line on one frame. The characteristics of turbulent shear flow were not measured, but the mean velocity at the center of the flume was measured by a propeller-type velocity meter.

3. Analysis of Experimental Results

3.1. Terminal Falling Velocity and Resistance Coefficient of Particle

For one of the properties of a particle falling in the turbulent shear flow, the terminal falling velocity was investigated. The terminal falling velocity in turbulent shear flow w_f was compared with that in still water. The particle sizes are from 4.5 mm to 7 mm, and the Reynolds number $R_e(=w_0 d/\nu)$ is of 10^3 order. In this region of the Reynolds number, the experimental result showed that the terminal falling velocity in turbulent shear flow is less than that in still water. Furthermore, we investigated the resistance coefficient of a particle falling in turbulent shear flow.

3.1.1. Terminal Falling Velocity of the Particle

The terminal falling velocity of the particle was evaluated from photographs in which a falling particle was shot on storoboscopic light. By knowing the trajectory of the particle for a given time interval, the falling velocity can be calculated. The mean value of the falling velocity was obtained by averaging more than ten data from photographs.

Table 2. The Values of w_0, w_f & C_D

Run	u_0 (cm/s)	H (cm)	Particle (cm)	w_f, w_0 (cm/s)	C_D
F-1	10.0	20.0	Bead	45.3	0.45
F-2	15.2		(0.5)	44.6	0.46
F-3	25.3			46.6	0.42
F-4	10.0	50.0		45.3	0.45
F-5	15.2			45.0	0.45
F-6	25.3			44.3	0.47
F-7	10.0	20.0	Gravel	29.9	0.96
F-8	15.2		(0.45)	31.7	0.94
F-9	25.3			30.8	1.00
F-10	10.0	50.0		31.7	0.95
F-11	15.2			31.1	0.98
F-12	25.3			30.9	1.00
F-13	25.3	50.0	B. (0.7)	54.1	0.44
F-14	25.3	50.0	I. (0.5)	96.8	0.48
F-15	0.0	60.0	B. (0.5)	49.7	0.38
F-16	0.0	60.0	G. (0.45)	32.6	0.90

For the same diameter bead, the variation of the calculated terminal falling velocity is very small. However, the falling velocities of gravel are different each time due to the effect of the shape of the gravel. The observed values of falling velocities in still water and in turbulent shear flow are shown in Table 2, in which w_0 is the value in still water and w_f in the turbulent shear flow. As shown in Table 2, there is a general trend such that w_f for every condition is less than w_0, and, the faster the mean flow velocity is, the less is w_f. In the author's experiments, the particle Reynolds number is limited in the order of 10^3, and so it cannot be concluded that the trend for w_f mentioned above is allowable for larger Reynolds numbers. This trend might be attributed to the magnus effect due to the interaction between the particle rotation and the mean flow. This problem should be thoroughly investigated in the future.

3.1.2. Resistance Coefficient of the Falling Particle

The resistance coefficient of the particle which is falling in still water or in turbulent shear flow is calculated by the following equation.[1)]

$$w_0,\ w_f=\left\{A\left(\frac{\sigma}{\rho}-1\right)\frac{g}{C_D}d\right\}^{1/2} \tag{1}$$

where A=coefficient related to a particle shape

ρ=density of water

σ=density of solid particle

g=acceleration of gravity

d=particle diameter

C_D=resistance coefficient

For the value of A, we used 4/3 for both beads and gravel because the value of A for a complex shape particle could not be easily determined. The value of C_D is shown in Table 2.

3.2. Distribution of Particles on the Bottom

The distributions of the particles at the bottom are plotted on the paper for the Gaussian plot, as shown in Fig. 2. In these plots, X-direction denotes longitudinal and streamwise direction and its origin is the point where the particle is dumped. Y-direction is in a transverse direction of the flume and its origin is the same point as that of X-axis. As shown in Fig. 1, the distributions of particles at the bottom can be recognized as Gaussian distributions for all cases, as well as in other runs. Thus, we can conclude that the distributions of particles at the bottom are Gaussian, independently of the dumping method, particle size and quality of materials.

For the elementary properties of settling particles, we take up the mean settling length of the particles (the longitudinal transport length), $\bar{X}$, and the standard deviation of the settling length σ_x. $\bar{X}$ and σ_x are defined as follows, respectively,

$$\bar{X}=\frac{1}{N\times m}\sum_{i=1}^{N\times m}X_i,\quad \sigma_x=\left\{\frac{1}{N\times m-1}\sum_{i=1}^{N\times m}(X_i-\bar{X})^2\right\}^{1/2} \tag{2}$$

where X_i is the settling length for particle i, and i varies from 1 to $N\times m$. Both $\bar{X}$ and σ_x were obtained by reading each value of the Gaussian plots given in Fig. 1. We

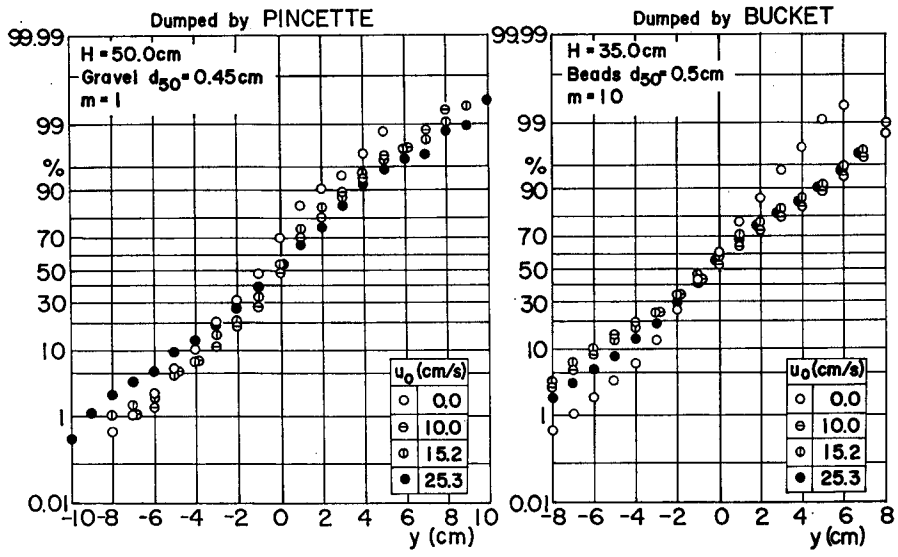

Fig. 1. Distribution of particles at the bottom.

expressed them as $\bar{X}_n$ and σ_{X_n}.

3.2.1. Mean Settling Length of Particles

Fig. 2 shows the relation between $(\bar{X}_n/d)$ and $(u/w_0 \cdot H/d)$ in the case of the P series experiments, while Fig. 3 shows the same relation in the B series experiments. As shown in both figures, $(\bar{X}_n/d)$ can be expressed as

$$\frac{\bar{X}_n}{d} = \frac{u}{w_0} \cdot \frac{H}{d} \tag{3}$$

where u is defined as $u=(1/H)\int_0^H u(z)dz$ and z is the vertical distance of which the origin is on a free surface.

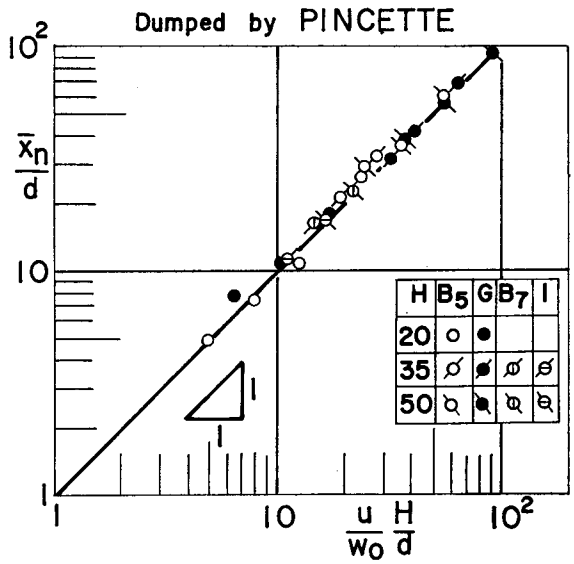

Fig. 2. Relations between (X_n/d) and (u/w_0) (H/d) in case of series P.

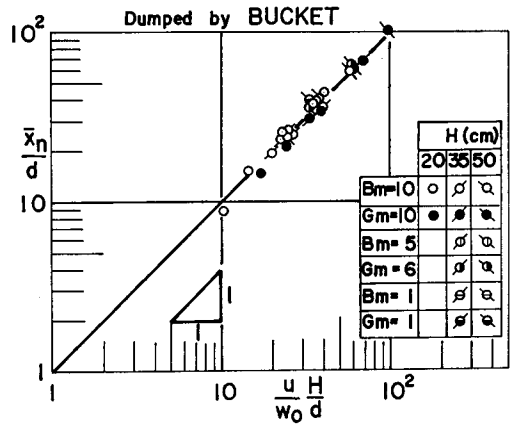

Fig. 3. Relations between (X_n/d) and (u/w_0) (H/d) in case of series B.

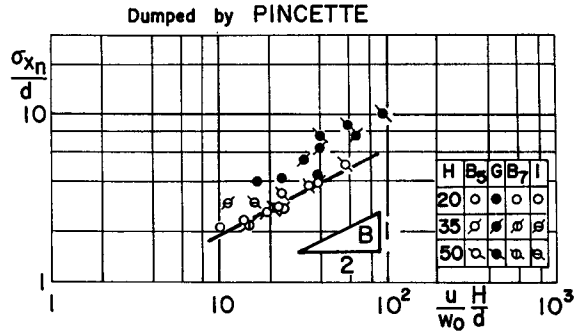

Fig. 4. Standard deviation of settling length in case of series P for bead.

Eq. (3) shows that $\bar{X}_n$ is not affected by either the settling method or the particle properties. From these results, it is concluded that the settling particles are transported with a mean flow velocity on the average.

3.2.2. Standard Deviation of Settling Length

Standard deviation σ_{X_n} shows different properties according to dumping methods. σ_{X_n} is related with the non-dimensional parameters (u/w_0) and (H/d), and the relationship between σ_{X_n} and these parameters is found to be dependent on the dumping method and the type of particles, as discussed in the following.

(1) Series P

Fig. 4 shows the relation between (σ_{X_n}/d) and $(u/w_0)(H/d)$ in both cases of sphere (based or iron) and gravel. As shown in this figure, σ_{X_n}/d for spherical particles can be expressed as,

$$\frac{\sigma_{X_n}}{d}=a_1\left(\frac{u}{w_0}\cdot\frac{H}{d}\right)^{1/2} \qquad a_1=\text{const. } (=0.6) \tag{4}$$

In case the of gravel, as shown in Fig. 5, σ_{X_n}/d can be expressed as

$$\frac{\sigma_{X_n}}{d}=a_2\left(\frac{u}{w_0}\right)^{1/2}\left(\frac{H}{d}\right)^{3/4}, \qquad a_2=\text{const. } (=0.42) \tag{5}$$

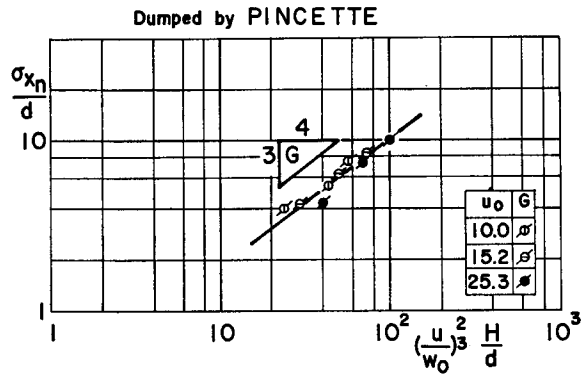

Fig. 5. Standard deviation of settling length in case of series P for gravel.

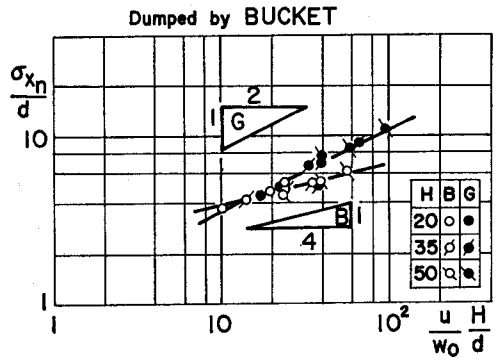

Fig. 6. Standard deviation of settling length in case of series B.

A qualitative explanation of the relationship between σ_{X_n} and these non-dimensional parameters is given in section 3.4.

(2) Series B

Fig. 6 shows the relation between (σ_{X_n}/d) and $(u/w_0)(H/d)$ in both cases of bead and gravel, and the relations can be expressed as

$$\text{Bead};\ \frac{\sigma_{X_n}}{d}=\alpha_3\left(\frac{u}{w_0}\cdot\frac{H}{d}\right)^{1/4},\qquad \alpha_3=\text{const.}\ (=2.2) \tag{6}$$

$$\text{Gravel};\ \frac{\sigma_{X_n}}{d}=\alpha_4\left(\frac{u}{w_0}\cdot\frac{H}{d}\right)^{1/2},\qquad \alpha_4=\text{const.}\ (=1.02) \tag{7}$$

Qualitative explanation about these relations will also be given later.

(3) Effects of the number of settling particles on standard deviation

We investigated what effects are provided on the value of σ_{X_n} by m, the number of settling particles in one trial. Fig. 7 shows the relation between the ratio of σ_{X_i} to $\sigma_{X_{10}}$, where σ_i is the standard deviation for i number of settling particles, and H/d with the parameter of u. For gravel, this ratio is always nearly one, and the effect of m on σ_X seems to be negligible. For bead, this ratio is approximately 0.85 and the number of

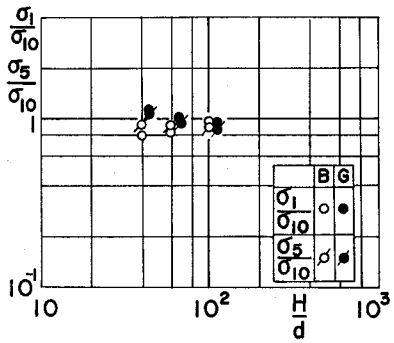

Fig. 7. Effect of number of settling particles at one trial on the value of σ_X.

settling particles, m, has some effect on the standard deviation σ_i, but this trend is dependent of H/d.

(4) Effects of dumping methods on standard deviation

The relations between the dumping methods and standard deviations are investi-

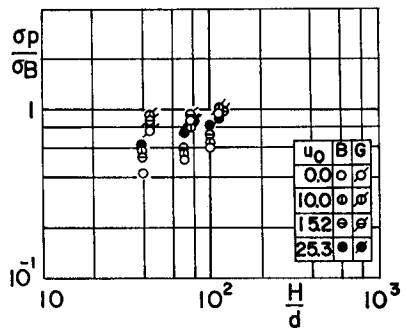

Fig. 8. Effect of settling method on the value of σ_X.

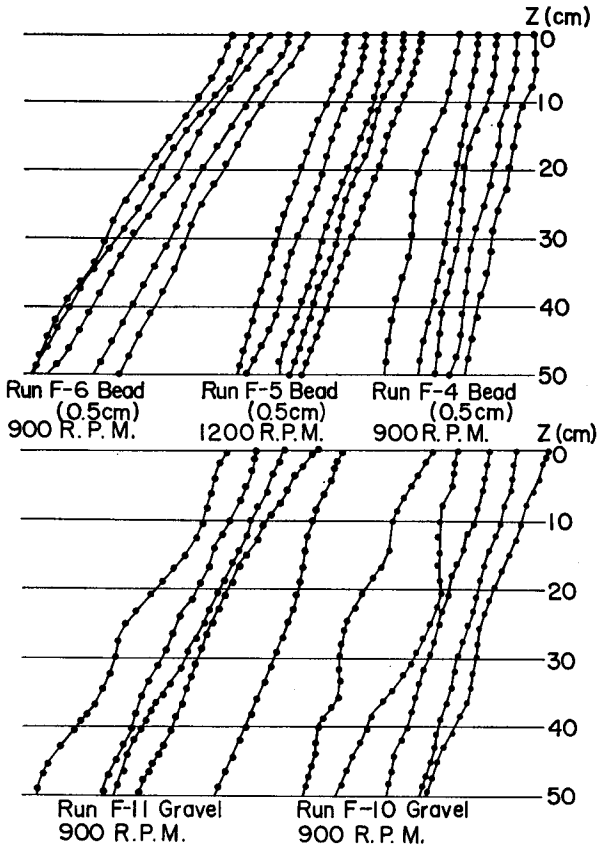

Fig. 9. Trajectories of settling particles in turbulent shear flow.

gated by evaluating the value of σ_P/σ_B, where σ_P indicates σ_{X_n} in series P and σ_B is σ_{X_n} in series B, as a function of H/d, as shown in Fig. 8. For both bead and gravel, σ_B is greater than σ_P, and this tendency is more remarkable for bead than gravel. The value of σ_P/σ_B approaches unity with an increase of H. This means that the effect of the settling method on σ_{X_n} is remarkable near the free surface where the particles are dumped, and becomes negligible with an increase of H. The spherical particle is more sensitive to the initial outer force, which is generated at the time when the particle is dumped, than an irregular shaped particle such as gravel.

3.3. Behavior of Particle Falling in Turbulent Shear Flow

In Fig. 9, the trajectories of falling particles, which have been obtained from storoboscopic photographs, are revealed. It is noticed from this figure that the settling particle falls with oscillating, being transported streamwise with a mean flow velocity. The wavelength of particle oscillation is about $20d$ to $30d$, and the amplitude of its oscillation is about $3d$, but these values are not constant and indicate a stochastic nature, each having a probability distribution.

In Fig. 10 the relation between $(\bar{X}_n/d)$ and $(u/w_0)(z/d)$ is shown, where z is the vertical distance from the free surface and $\bar{X}_n$ is the settling length when the particle

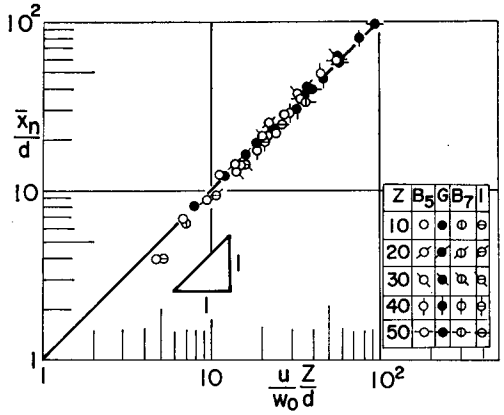

Fig. 10. Relations between (X_n/d) and (u/w_0) (z/d) in case of series F.

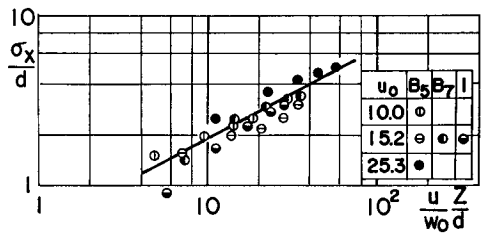

Fig. 11. Standard deviation of settling length for spherical particle.

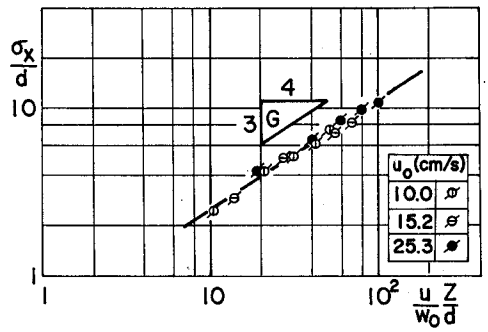

Fig. 12. Standard deviation of settling length for gravel.

has fallen to z. As shown in Fig. 10, $\bar{X}_n$ is proportional to both u and z, and is inversely proportional to w_0.

Fig. 11 shows the relation between (σ_{X_n}/d) and $(u/w_0)(z/d)$ for bead. Although data in the figure indicate some scattering, (σ_X/d) can be expressed as follows:

$$\frac{\sigma_X}{d}=\alpha_1\left(\frac{u}{w_0}\cdot\frac{H}{d}\right)^{1/2}, \qquad \alpha_1=\text{const.} \tag{4'}$$

where σ_X is the standard deviation of X at z.

For gravel, as shown in Fig. 12, (σ_X/d) can be expressed as

$$\frac{\sigma_X}{d}=\alpha_2\left(\frac{u}{w_0}\right)^{1/2}\left(\frac{H}{d}\right)^{3/4}, \qquad \alpha_2=\text{const.} \tag{5'}$$

The properties of $\bar{X}$ and σ_X in the F series experiment are equal to those in series P. In both series, the same dumping method by pincette was used. The turbulent structure is different for the P series and the F series, even if the mean flow velocity is the same for both cases, because of different depths. $\bar{X}$ and σ_X at 20 cm and 35 cm depths, which are obtained from particle trajectories shown in Fig. 9 for the F series, are compared with the values in the P series for the same depths, respectively. In spite of different turbulent structures, the property of $\bar{X}$ and σ_X are the same in both cases. This is caused by the fact that, because the particle diameter is comparatively large, the falling particle is not affected by a small scale turbulence but rather by large scale parameters such as the mean flow velocity and the vorticies occurring behind the particle itself.

3.4 General Considerations for Experimental Results of Standard Deviation

In this section, the properties of σ_X obtained at 3-2 are discussed qualitatively by taking account of the following four casues of the variations of X:

i) Stochastic properties of the flow such as turbulent fluctuation
ii) Vorticies generated behind the falling particle
iii) Shape factor of the particle

iv) Initial disturbance induced at the beginning of dumping work

The effects of i) and ii) are typically shown in the P-series experiments (P-1～12 in case of bead.) The behavior of the particle due to i) and ii) is analogous to Brownian motion and therefore the standard deviation will be proportional to $H^{1/2}$.

The effects of iii) appear in the P-series experiments of gravel (P-13～24). Since the settling velocity w_0 is affected by shape factors, standard deviation σ_X depends upon the deviation of w_0 for the constant mean flow velocity. Also, since $X \propto (u/w_0)H$, σ_X is to increase with H, if the value of w_0 is different for each particle. At last, σ_X due to iv) is independent of H, because this deviation is caused only by the dumping condition.

When a bead is dumped by a pincette, the factors causing the deviation X are i) and ii), and thus σ_X increases with $H^{1/2}$. But when the same bead is dumped by a bucket, the deviation of X caused by iv) is not neglected, and σ_X tends to increase with less power than 1/2 of H.

For gravel, if it is dumped by a pincette, the deviation of X is caused by i), ii) and iii) and σ_X tends to increase with H^{α}, where α is the value from 1/2 to 1. When the gravel is dumped by a bucket, all factors of i)～iv) have an influence on the deviation of X, and σ_X has a possibility of increasing with H^{β}, where β is the value from 0 to 1. When the particles are dumped with a knot, σ_X caused by iii) tends to be smaller, and this tendency is thought to be important for estimating σ_X.

4. Stochastic Model of Settling Particles

4.1 General Scope of Modelling

Most of the current studies on the behavior of settling particles are cases of particles settled in still water. Furthermore, the distribution of settling particles at the bottom, which are dumped from an appointed position on the free surface, has hardly been investigated. Yanai[1] considered the movement of particles as a random walk, and concluded that the distribution of particles on the bottom is binomial and the standard deviation σ increases with $H^{1/2}$. Kikkawa et al.[2] resolved the distributional property of a settling particle by using the concept of a stochastic differential equation. They said that the standard deviation σ of the settling particles increased with $z^{1/2}$, in which z was the vertical distance from the settled point. Li et al.[3] investigated the mean settling length of a particle in turbulent shear flow and its distribution function, but the settling particle was so small that it moved together with the sorrounding fluid turbulence.

There is no study dealing with the properties of a settling particle when the Reynolds number is greater than 10^2, because in most cases small particles were used and the flow surrounding the particle was limited to such cases where the Stokes' law could be adapted

Here, we have investigated the behavior of large particles in turbulent shear flow, with the particle sizes being from 4.5 mm to 7 mm, and the Reynolds number $R_*(=w_0$

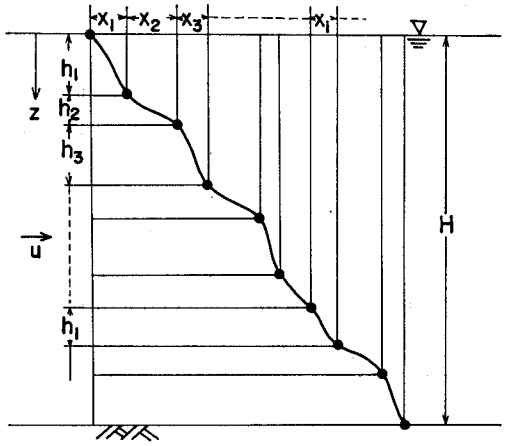

Fig. 13. Definition ksetch of particle movements.

d/ν) is in the order of 10^3.

The behavior of a settling particle is so complex and uncertain that it is difficult to obtain its dynamical and deterministic description. Hence, in describing its behavior, the stochastic approach should be applied. As shown in Fig. 10, the motion of a settling particle can be regarded as a stochastic process in which both the duration and the amplitude of a particle oscillation are random variables, each having a probability distribution. Therefore, we propose the stochastic model to find the relations between $\bar{X}$, σ_X and H, u, w_0.

4.2 Structure of Stochastic Model

The trajectory of a settling particle is shown schematically in Fig. 13, in which the dotted points indicate the position where the settling particle changes its direction due to vortices behind particle and large scale turbulence. X_i is the horizontal distance and h_i is the vertical distance between the (i-1) th spot and the i-th spot, in which i starts at the free surface. The duration, in which the particle moves from the (i-1)-th spot to the i-th spot, is defined as T_i, and T_i is expressed as $T_i=h_i/w_f$, where w_f is the terminal fall velocity of the particle in the shear flow.

As mentioned in 3-2, the particle is streamwisely transported with an almost mean flow velocity, and then the transported distance during T_i can be expressed as $c_1 u\, T_i$($c_1=w_f/w_0$), unless the falling particle is influenced by the vortices or turbulence. Actually, the transported distance is deviated by the above causes, and length of deviation Δx_i is represented as

$$\Delta X_i=X_i-c_1 u T_i \tag{8}$$

If $X(z)$ is defined as the horizontal transported distance at the time when the particle has fallen to z, then $X(z)$ is given by

$$X(z)=\sum_{i=1}^{N(t)} X_i=u\frac{z}{w_0}+\sum_{i=1}^{N(t)}\Delta x_i \tag{9}$$

in which $N(t)$=the number of oscillating steps before the particle falls to z and $t=z/w_0$. $N(t)$ is regarded as a random variable, while Δx_i is also a random variable. For convenience, we define ΔX as

$$\Delta X=\sum_{i=1}^{N(t)}\Delta x_i \tag{10}$$

Both $N(t)$ and Δx_i are random variables and independent of each other, and thus ΔX is regarded as a compound stochastic process.

Now, the mean value and the variance of $X(z)$ are respectively given as follows:

$$E[X(z)]=E\left[u\frac{z}{w_0}\right]+E[\Delta X]$$

$$\begin{aligned} V[X(z)]&=E[X^2(z)]-E[X(z)]\\ &=E\left[\left(u\frac{z}{w_0}\right)^2+2\left(u\frac{z}{w_0}\right)\Delta X+\Delta X^2\right]-E^2[X(z)]\\ &=E\left[\left(u\frac{z}{w_0}\right)^2\right]+2E\left[\left(u\frac{z}{w_0}\right)\Delta X\right]+E[\Delta X^2] \end{aligned} \tag{11}$$

$$-E^2\left[\left(u\frac{z}{w_0}\right)\right]-2E\left[u\frac{z}{w_0}\right]\cdot E[\Delta X]-E^2[\Delta X] \tag{12}$$

In order to make clear the relationships between $E[X(z)]$, $V[X(z)]$ and z, the statistical properties of both ΔX and (uz/w_0) for z must be given. Firstly, the properties of ΔX for z will be investigated. According to the theory of the compound stochastic process,[4] the mean value and the variance of ΔX can be expressed as

$$E[\Delta X]=E[N(t)]\cdot E[\Delta x_i] \tag{13}$$

$$V[\Delta X]=V[N(t)]\cdot E^2[\Delta x_i]+E[N(t)]\cdot V[\Delta x_i] \tag{14}$$

Therefore, the problem comes to the stochastic properties of Δx_i and $N(t)$. As to Δx_i, the following can be assumed on the basis of the trajectories of the falling particles as shown in Fig. 9:

i) Δx_i shows either a plus or minus value sequentially or randomly until the particle reaches the bottom.

ii) Each amplitude of particle fluctuation is independent.

Now, let x_i^+ and x_i^- be the amplitude of particle fluctuation for streamwise and counter-streamwise, respectively. Fig. 14 shows the distributions of both x_i^+ and x_i^-, which were obtained from observed trajectories for several runs. Although some scatter exists, almost the same distributions are obtained for both x_i^+ and x_i^-, so that their mean values and variances become nearly the same. For the stochastic model of Δx_i, therefore, the following two models are presented. Model 1 is such that x_i^+

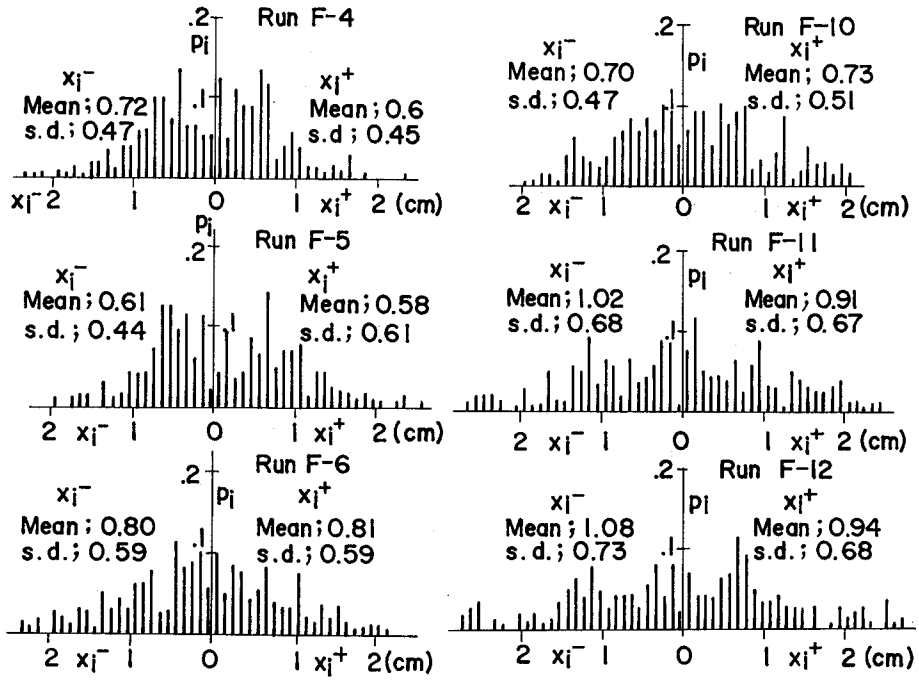

Fig. 14. Distribution of x_i^+ and x_i^-.

and x_i^- exactly occur alternatively, and Model 2 is such that the direction of Δx_i is random. According to Model 1, Eq. (10) is rewritten as

$$\Delta X=\sum_{i=1}^{N(t)}\Delta x_i=\sum_{i=1}^{1/2N(t)}(x_i^+-x_i^-), \qquad (x_i^+\geqq 0,\ x_i^-\geqq 0) \tag{15}$$

When x_i is defined as $x_i=x_i^+-x_i^-$, $E[x_i]$ and $V[x_i]$ become in consideration of the relations that $E[x_i^+]=E[x_i^-]$ and $V[x_i^+]=V[x_i^-]$,

$$E[x_i]=E[x_i^+]-E[x_i^-]=0 \tag{16}$$

$$V[x_i]=V[x_i^+]+V[x_i^-]=2V[x_i^+] \tag{17}$$

According to Model 2, the probability distributional function of Δx_i, $g(\Delta x_i)$, is symmetrical for the $g(\Delta x_i)$ axis, and, letting $f(x_i^+)$ be the probability density function of x_i^+, $g(\Delta x_i)$ is expressed as $g(\Delta x_i)=1/2\cdot f(|\Delta x_i|)$. Then, $E[\Delta x_i]$ and $V[\Delta x_i]$ are written as

$$E[\Delta x_i]=0 \tag{18}$$

$$V[\Delta x_i]=E[x_i^{+2}]=V[x_i^+]+E^2[x_i^+] \tag{19}$$

Next, we consider the stochastic properties of $N(t)$. If the duration T_i is an independently random variable, $N(t)$ becomes the renewal process. According to the renewal process theory[4] it is recognized that, if $E[T_i]=\tau$ and $V[T_i]=\sigma_\tau$,

$$E[N(t)]=\frac{1}{\tau}t \qquad \text{for } t\to\infty \tag{20}$$

$$V[N(t)]=\frac{\sigma_\tau^2}{\tau^3}t \qquad \text{for } t\to\infty \tag{21}$$

Since $t=z/w_f$, Eq. (20) and Eq. (21) are rewritten as

$$E[N(t)]=\frac{1}{\tau}\cdot\frac{z}{w_f} \qquad \text{for } t\to\infty \tag{22}$$

$$V[N(t)]=\frac{\sigma_\tau^2}{\tau^3}\cdot\frac{z}{w_f} \qquad \text{for } t\to\infty \tag{23}$$

According to Eqs. (16), (17) and (22), $E[\Delta X]$ and $V[\Delta X]$ for Model 1 are given as

$$E[\Delta X]=E[\tfrac{1}{2}N(t)]\cdot E[x_i]=0 \tag{24}$$

$$\begin{aligned}V[\Delta X]&=V[\tfrac{1}{2}N(t)]\cdot E^2[x_i]+E[\tfrac{1}{2}N(t)]\cdot V[x_i]\\&=E[\tfrac{1}{2}N(t)]\cdot V[x_i]\\&=\frac{\sigma_\tau^2}{\tau^3}\cdot\frac{1}{w_f}V[x_i^+]\cdot z \qquad \text{for } z\to\infty\end{aligned} \tag{25}$$

According to Eqs. (18), (19) and (23), $E[\Delta X]$ and $V[\Delta X]$ for Model 2 are given as

$$E[\Delta X]=E[N(t)]\cdot E[\Delta x_i]=0 \tag{26}$$

$$\begin{aligned}V[\Delta X]&=V[N(t)]\cdot E^2[\Delta x_i]+E[N(t)]\cdot V[\Delta x_i]=E[N(t)]\cdot V[\Delta x_i]\\&=E[N(t)]\cdot\{V[x_i^+]+E^2[x_i^+]\}\\&=\frac{\sigma_\tau^2}{\tau^3}\cdot\frac{1}{w_f}\{V[x_i^+]+E^2[x_i^+]\}\cdot z \qquad \text{for } z\to\infty\end{aligned} \tag{27}$$

The stochastic properties of uz/w_0 are dependent upon those of w_0 which are related to the kind of particles. In the case of bead, the particles have the same size and shape for all runs, and so w_0 seems to be constant and $V[uz/w_0]$ is zero. But, in the case of gravel, the shapes of the particles are different from each other even for the same diameter, and thus w_0 is regarded as a random variable and $V[uz/w_0]$ is not zero. In the following, the properties of $E[X(z)]$ and $V[X(z)]$ for bead and gravel will be investigated.

4.3 Application of Stochastic Model to Experimental Results

In the case of bead dumped by a pincette, the initial deviation of X is negligible, so $E[X(z)]$ and $V[X(z)]$ can be represented by Eqs. (11) and (12), respectively. In these equations the value of (uz/w_0) is considered to be constant, and can be rewritten as

$$E[X(z)]=\frac{u}{w_0}z+E[\Delta X] \tag{28}$$

$$V[X(z)]=E[\Delta X^2]-E^2[\Delta X]=V[\Delta X] \tag{29}$$

Then, for Model 1, $E[X(z)]$ and $V[X(z)]$ are expressed as

$$E[X(z)]=\frac{u}{w_0}z \tag{30}$$

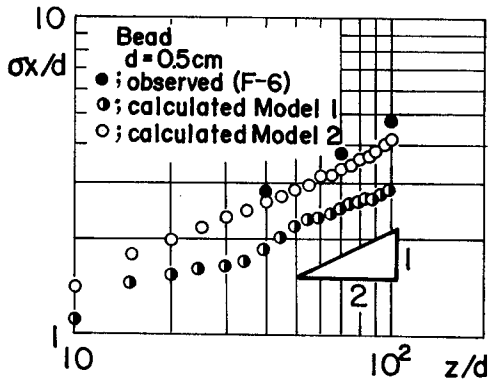

Fig. 15. Variation of σ_X simulated by stochastic models for bead.

$$V[X(z)]=\beta_1 V[x_i^+]z \qquad \text{for } z\to\infty \tag{31}$$

And, for Model 2,

$$E[X(z)]=\frac{u}{w_0}z \tag{32}$$

$$V[X(z)]=\beta_1\{V[x_i^+]+E^2[x_i^+]\}z \qquad \text{for } z\to\infty \tag{33}$$

In both Models 1 and 2, $E[X(z)]=uz/w_0$ and $V[X(z)]\propto z$. These statistical properties explain qualitatively the experimental results for bead settled by a pincette.

By using these stochastic models, we attempted to simulate the behavior of the settling particle. An example of the results is shown in Fig. 15 for the case of run F-6. In this simulation, the observed values of $E[x_i^+]$ and $V[x_i^+]$ shown in Fig. 14 were used. From Fig. 15 it is recognized that Model 2 is better fitted to the experimental results than Model 1. This fact suggests that the direction of the fluctuation of the particle is random.

Next, we investigate the case where w_0 is a random variable such as gravel. The distribution of w_0 is considered to be a gamma distribution or a logarithmic normal distribution. For the gamma distribution, the distribution function $F(w_0)$ is given by

$$F(w_0)=\frac{\lambda(\lambda w_0)^{n-1}}{(n-1)!}\cdot\exp(-\lambda w_0) \qquad (w_0\geqq 0) \tag{34}$$

Then, $E[w_0]$ and $V[w_0]$ are expressed as, respectively,

$$E[w_0]=\frac{n}{\lambda}, \qquad V[w_0]=\frac{n}{\lambda^2} \tag{35}$$

In this case the distribution of $X(=uz/w_0)$ is given as

$$F'[X]=\frac{uz}{X^2}\cdot F\left(\frac{uz}{X}\right)=\frac{\lambda uz}{X}\cdot\frac{\left(\frac{uz}{X}\right)^{n-1}}{(n-1)!}\cdot\exp(-\lambda uz/X) \tag{36}$$

Thus, $E[X]$ and $V[X]$ are represented as

$$E[X]=\frac{\lambda uz}{n-1} \tag{37}$$

$$V[X]=\frac{\lambda^2(uz)^2}{(n-1)^2(n-2)} \tag{38}$$

By using Eq. (35), Eqs. (37) and (38) are transformed to

$$E[X]=\frac{uz}{E[w_0]}\cdot\frac{n}{n-1} \tag{39}$$

$$V[X]=\frac{(uz)^2}{V[w_0]}\cdot\frac{n}{(n-1)^2(n-2)} \tag{40}$$

For example, if $n=100$ and $\lambda=100/w_0$, then $E[w_0]=w_0$ and $V[w_0]=0.01w_0$, and we can obtain that $E[X]=(100/99)\cdot(uz/w_0)\simeq uz/w_0$ and $V[X]=(100^2/99^2\times 98)\cdot(uz/w_0)\simeq 0.01(uz/w_0)$. The latter relation shows that the deviation of X due to the randomness of w_0 increases with z^2. According to the above consideration, $E[X(z)]$ and $V[X(z)]$, in the case where w_0 is a random variable, are given as follows:

$$E[X(z)]=E\left[\frac{u}{w_0}z\right]+E[\Delta X]=\frac{u}{w_0}\cdot z \tag{41}$$

$$V[X(z)]=V\left[\frac{u}{w_0}z\right]+V[\Delta X]=\frac{K_1}{V[w_0]}\cdot(uz)^2+V[\Delta X] \quad K_1\text{; constant} \tag{42}$$

Fig. 16 shows the simulated result for the run F-12 in which Model 2 is applied for Δx_i. For the case where w_0 is regarded as a random variable and the standard deviation of w_0 is $E[w_0]/10$, the simulated curve gives a good agreement with the experimental result.

On the other hand, when the particles are dumped by bucket, the deviation of $X(z)$ at the starting point of settling, i.e. at $z=0$, cannot be neglected. This deviation is

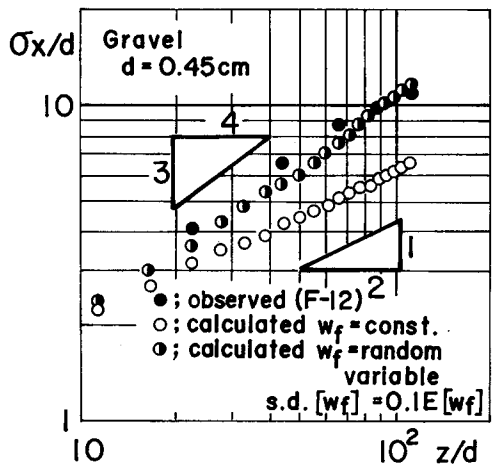

Fig. 16. Variation of σ_X simulated by stochastic models for gravel.

independent of z and hence Eq. (9) is written as

$$X(z)=\sum_{i=1}^{N(t)} X_i+X_{ini} \tag{9'}$$

in which X_{ini} is the fluctuation due to the initial effect and $E[X_{ini}]=0$ and $V[X_{ini}]=\alpha_1$ where α_1 is a constant. Because X_{ini} is considered to be independent of uz/w_0 or ΔX, $E[X(z)]$ and $V[X(z)]$ are represented as

$$E[X(z)]=E\left[\frac{u}{w_0}z\right]+E[\Delta X]+E[X_{ini}] \tag{11'}$$

$$V[X(xz)]=V\left[\frac{u}{w_0}z\right]+V[\Delta X]+V[X_{ini}] \tag{12'}$$

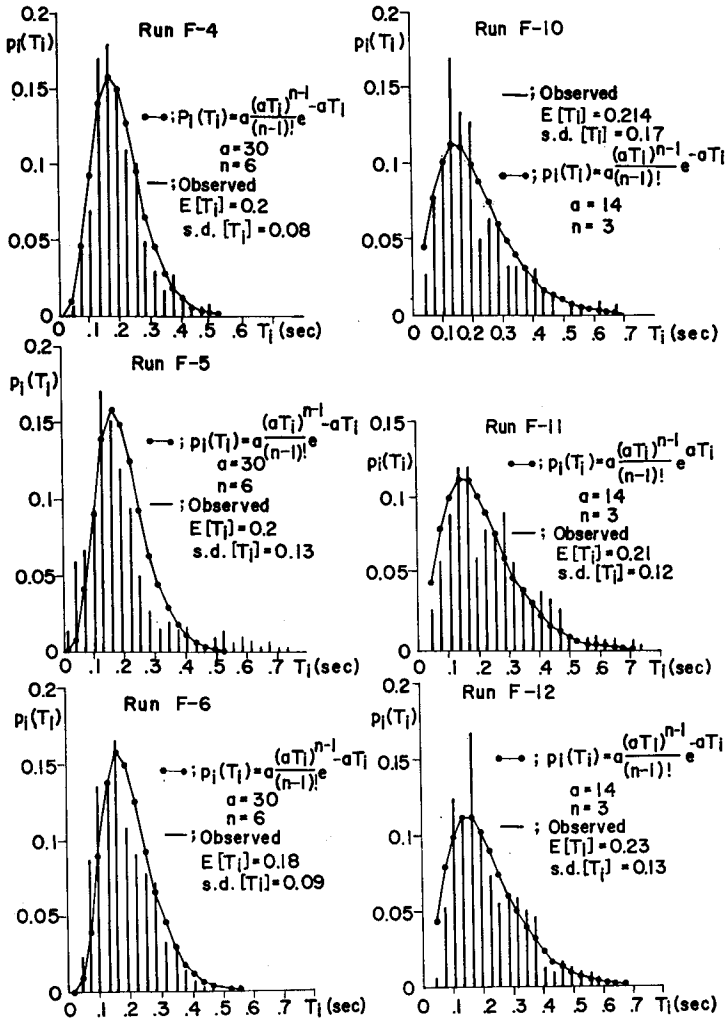

Fig. 17. Distribution of duration of particle oscillation, T_i.

By using Eqs. (32), (33) and (40) which define the statistical properties of uz/w_0 and ΔX, the relations $E[X(z)]$ and $V[X(z)]$ to z are given as

$$E[X(z)]=A\cdot z \tag{43}$$

$$V[X(z)]=B\cdot z^2+C\cdot z+D \tag{44}$$

in which A, B, C and D are the coefficients. If Eq. (44) can be approximated by the function of C_1z^η (C_1: coefficient), the value of η changes from zero to two, according to the values of B, C and D. If the value of D becomes relatively large compared with B and C, η becomes smaller, and if B is relatively large compared with C and D, η becomes larger. In our experiment, when beads are dumped by bucket, the result that $V[X(z)] \propto z$ has been obtained, but for gravel the result is such that $V[X(z)]\propto z^{3/2}$.

As mentioned above, we could explain the experimental results by using the concepts of the stochastic process. But, these descriptions are limited to the qualitative one, and so we need to make clear the statistical properties of $[T_i]$ and $[\Delta x_i]$, not only qualitatively but also quantitatively.

Fig. 17 shows the distributions of the duration T_i for several experiments. As shown in the figure, in spite of the difference of u, almost the same distributions are shown for the same particles. For reference, the gamma distribution curves are shown in the figures. On the other hand, as shown in Fig. 14, the distributions of x_i^+ or x_i^- are different by the mean flow velocity even for the same particle. In the case of gravel, the larger u_0 is, the larger $E[x_i^+]$ and $V[x_i^-]$ are. But, at present, the knowledge for $[T_i]$ and $[\Delta x_i]$ is limited, and it is necessary to obtain further information about the relationships between these parameters and flow conditions.

5. Conclusion

In this study, some statistical properties of solid particles, which settled in the turbulent shear flow, have been investigated experimentally and theoretically. The results obtained here are summarized as follows:

(1) The mean settling length the flow direction, $E[X(z)]$, is given by uz/w_0 and $E[Y(z)]$ in the transversal direction is nearly zero for any flow condition.

(2) The standard deviation of the settling length, $\sigma_X(z)$,depends upon u, w_0 and the settling method, and the trend of its variation differs according to the type of the particles.

(3) The behavior of the settling particle can be regarded as the compound stochastic and process and can be fairly explained by the stochastic model qualitatively. In order to obtain the quantitative description of a settling particle, it is neces sary to make clear the statistical properties of $[T_i]$ and $[\Delta x_i]$ relating to the flow conditions.

Acknowledgement

The authors wish to express there deep gratutude to T. Ikezoe, a graduate student of Kyoto University, for his kind help in carrying out these experiments.

References

1) Yanai, K., Proc. of JSCE, No. 69 (1960).
2) Kikkawa, H., Fukuoka, S. and Yoshikawa, K., Proc. of the 20th J.C.H., JSCE, 115 (1976).
3) Li, R. M. and Shen, H. W., Proc. of ASCE, HY 7, 917 (1975).
4) Fujisawa, T., Probability and Statistics, Nippon Riko Shuppan Kai.
5) Alger, G. R., Proc. of ASCE, HY 3, 721 (1968).